International Journal of Nanomedicine

Dovepress

open access to scientific and medical research

Open Access Full Text Article

ORIGINAL RESEARCH

Green Synthesis and Characterization of Silver Nanoparticles Using *Moringa Peregrina* and Their Toxicity on MCF-7 and Caco-2 Human Cancer Cells

Khaled Saeed Yousef Al Baloushi[1], Annadurai Senthilkumar[1,2], Karthishwaran Kandhan[1], Radhakrishnan Subramanian[1], Jaleel Kizhakkayil[3], Tholkappiyan Ramachandran[4,5], Safa Shehab[6], Shyam Sreedhara Kurup[1], Mohammed Abdul Muhsen Alyafei[1], Ayesha Salem Al Dhaheri[3], Abdul Jaleel[1]

[1]Department of Integrative Agriculture, College of Agriculture and Veterinary Medicine, United Arab Emirates University, Al Ain, United Arab Emirates; [2]PG and Research Department of Botany, Kandaswami Kandar's College, Velur, TN, India; [3]Department of Nutrition & Health Sciences, College of Medicine and Health Sciences, United Arab Emirates University, Al Ain, United Arab Emirates; [4]Department of Physics, Khalifa University of Science and Technology, Abu Dhabi, United Arab Emirates; [5]Department of Physics, Saveetha School of Engineering, Saveetha Institute of Medical and Technical Science, Saveetha University, Chennai, TN, India; [6]Department of Human Anatomy, College of Medicine and Health Sciences, United Arab Emirates University, Al Ain, United Arab Emirates

Correspondence: Abdul Jaleel, Tel +971-3-713-4576, Email abdul.jaleel@uaeu.ac.ae

Introduction: The synthesis of nanoparticles using naturally occurring reagents such as vitamins, sugars, plant extracts, biodegradable polymers and microorganisms as reductants and capping agents could be considered attractive for nanotechnology. These syntheses have led to the fabrication of limited number of inorganic nanoparticles. Among the reagents mentioned above, plant-based materials seem to be the best candidates, and they are suitable for large-scale biosynthesis of nanoparticles.

Methods: The aqueous extract of *Moringa peregrina* leaves was used to synthesize silver nanoparticles. The synthesized nanoparticles were characterized by various spectral studies including FT-IR, SEM, HR-TEM and XRD. In addition, the antioxidant activity of the silver nanoparticles was studied *viz*. DPPH, ABTS, hydroxyl radical scavenging, superoxide radical scavenging, nitric oxide scavenging potential and reducing power with varied concentrations. The anticancer potential of the nanoparticles was also studied against MCF-7 and Caco-2 cancer cell lines.

Results: The results showed that silver nanoparticles displayed strong antioxidant activity compared with gallic acid. Furthermore, the anticancer potential of the nanoparticles against MCF-7 and Caco-2 in comparison with the standard Doxorubicin revealed that the silver nanoparticles produced significant toxic effects against the studied cancer cell lines with the IC_{50} values of 41.59 (Caco-2) and 26.93 (MCF-7) µg/mL.

Conclusion: In conclusion, the biosynthesized nanoparticles using *M. peregrina* leaf aqueous extract as a reducing agent showed good antioxidant and anticancer potential on human cancer cells and can be used in biological applications.

Keywords: plant-based nanoparticles, silver nanoparticles, *Moringa peregrina*, anticancer, antioxidant activity

Introduction

The utilization of nanotechnology in arid land plant research will be a promising tool to exploit underutilized plants. Nanotechnology gives an extensive innovative platform to the investigation and conversion of the biological system and serves as an inspirational design involving biological constituents.[1] These days, nanotechnology has seen a lot of changes, for example, potential procedures utilized, and the use of various physicochemical agents, involving nano-sized metal particles to manufacture new medications, which make them fruitful for application in natural and pharmaceutical ventures.[2] Nanoparticles play a vital role in medicine, chemistry, electronics and catalysis. The syntheses

Received: 7 December 2023
Accepted: 1 April 2024
Published: 30 April 2024

of nanoparticles are carried out by three different methods – chemical, physical and biological. Green synthesis of silver nanoparticles from plants is one of the most interesting areas because it is rapid, efficient and nontoxic, economical, and environment friendly.[3]

Silver nanoparticles have brought in extensive enthusiasm because of their numerous interesting properties and applications. Plants offer a superior stage for nanoparticle synthesis as they have non-poisonous mixes and consist of natural capping agents. Silver nanoparticles are comprehensively utilized in various zones, particularly in pharmaceutical and clinical fields.[4] Nanoparticles are ordinarily utilized as a drug delivery system as they are useful in not just controlling the molecule size, surface region, and properties of the drug, but additionally help in conveying the pharmacologically dynamic operators to the site of activity at a rational rate and dose of the drug.[5] Silver is a compelling antibacterial agent and displays low toxicity which is important, particularly in the treatment of burn wounds. Nanocarriers are utilized as drug delivery systems in light of their exceptional characteristics, for example, high drug loading capacity, biodegradability, site-specific delivery mechanism and not affecting normal cells and tissues.[6] Silver nanoparticles have been explored for their cytotoxic action as they display various degrees of in vitro toxicity.[7]

Especially, nanoparticles are most commonly utilized in the clinical field of drug delivery systems, targeted therapy, and gene therapy due to the result of their simplicity of control and attributes, accomplished by dynamic medication focusing on parenteral organization.[8] Green synthesis of nanoparticles utilizing the plants that have restorative worth offers us new types of drugs which have been viably used in ancient medicine. The drugs originating from plants have less harmful reactions just as they are affordable and more viable.[9] Several studies have reported the utilization of plants for the synthesis of metal nanoparticles like silver, gold, copper, and composites.[10–13]

Moringa species is one of the most useful trees in the tropics and subtropics of Asia and Africa, with multiple uses. *Moringa peregrina* belongs to the family Moringaceae and native to the arid and semi-arid regions.[14] It is a fast-growing, deciduous tree growing up to 10 m in height. The leaves are imparipinnate with early deciduous leaflets, flowers are bisexual, yellowish white to pink in color. The leaves of the plant are an excellent source of minerals, amino acids and proteins.[15] Also, *M. perigrina* has many other phytochemicals such as flavonoids, alkaloids, glycosides, tannins, proanthocyanidins, lignans, terpenoids, phenylpropanoids, proteins, resins, furocoumarins and naphthodianthrones.[16] The plant was previously studied for phytochemical compositions and their biological activities. Even though the plant has wide phytochemical diversity, there was no study on the *M. peregrina*-mediated biosynthesis of nanoparticles. Therefore, the present study focused on the synthesis and characterizes the silver nanoparticles using *M. peregrina* leaf extract and their antioxidant and anticancer activities.

Materials and Methods

Plant Materials

The fresh leaves of *Moringa peregrina* (Forssk.) Fiori. were collected from Al Foah [24°21'31.139" N 55°47'57.239" E (Altitude 303 M)], Al Ain, UAE. The herbarium of the plant was identified and authenticated by Dr. Mohamed Taher Moussa (Botanist Incharge and Lab Specialist) and the voucher specimen (UAEU-NH14688) was deposited at the National Herbarium of the Biology Department, College of Science, United Arab Emirates University, UAE. All experiments are done as per the institutional guidelines. There are no further approvals required to conduct research on plant materials.

The samples were initially washed with tap water and then washed with 10% sodium hypochlorite to prevent contamination. Finally, the fresh leaf samples were rinsed thoroughly with distilled water and utilized for extract preparation.

Preparation of *Moringa* Aqueous Extract and Synthesis of Silver Nanoparticles

For the preparation of *M. peregrina* leaf aqueous extract, 20 gm of leaf powder was mixed with 200 mL of deionized water and kept in a water bath (60 °C) for 20 mts. The extract was filtered after cooling with Whatman No. 1 filter paper and used for the green synthesis of nanoparticles. For the silver nanoparticles synthesis, the aqueous extract (2 mL) of *M. peregrina* leaves was added into an Erlenmeyer flask containing 60 mL of 1 mM silver nitrate ($AgNO_3$-Sigma-

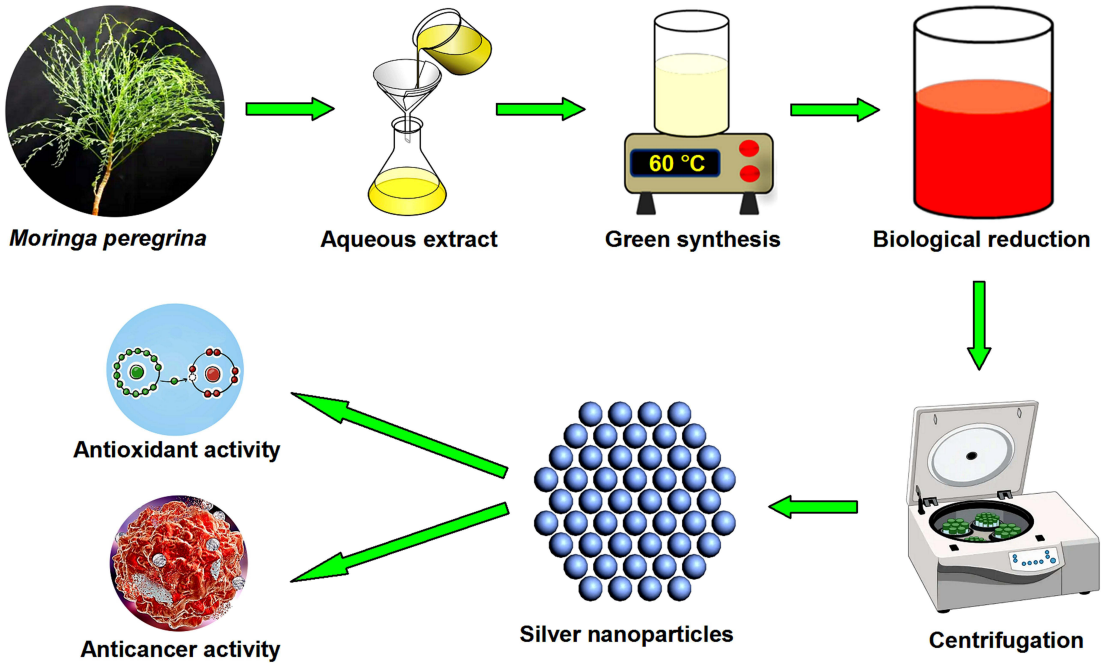

Figure 1 Schematic diagram of biosynthesis of *Moringa peregrina* leaf extract mediated AgNPs and its biological activity.

Aldrich) solution and kept on a magnetic stirrer with a hot plate for incubation for 2 h at 50°C.[17] To minimize the photoactivation of silver nitrate, the reaction process was carried out in a darkroom condition. After incubation, the solution color turned into a reddish-brown (Figure 1). The change of color of the reaction solution was detected in the characterization of the silver nanoparticles. Finally, the solution was centrifuged at 15,000 rpm for 20 min. The transparent solution was discarded, and the pellet of silver nanoparticles was collected. The solution was dried in the hot air oven between 45 and 50°C to obtain pellets.

Characterization of Silver Nanoparticles

FT-IR Analysis

FT-IR spectra were recorded with wave numbers ranging from 400 to 4000 cm^{-1} for the *Moringa peregrina* leaf extract mediated silver nanoparticles (AgNPs) using Avatar–370 FT-IR spectrometer using KBr (pellet form) to record the IR spectra.

SEM Analysis

The synthesized AgNPs were analyzed by scanning electron microscope – quanta 200 FEG (Resolution: 1.2 nm Au particle separation on a carbon substrate magnification: from a min of 12× to greater than 1,00,000×) an instrument attached with EDX analyzer (JEOL JED-2300) accelerating voltage of the analysis station at 20 keV.

HR-TEM Analysis

The aqueous solution of AgNPs was poured as a drop on the carbon-coated Cu grid and allowed to dry at ambient temperature for 2 hours. The synthesized AgNPs were viewed under High-Resolution TEM (FEI Spirit G2 BioTwin, Tecnai (200 kV), TEM, Eindhoven, Netherlands), and images were taken at a different magnification at HT = 100 kV Spot Size = 1 Magnification = 50–100 nm (as per image magnification) with Veleta camera (Olympus Soft Imaging Solutions). Thin Foil Apertures: Condenser Aperture = 100 µm Objective Aperture = 40 µm to view lattice resolution of 0.14 nm and point-to-point resolution of 0.19 nm at 200 kV.

XRD Analysis

The XRD technique was used to check the formation of mono-phase compounds. *Moringa peregrina*-mediated AgNPs were washed completely in distilled water (triple), centrifuged and dried (at room temperature). The purified AgNPs were

analyzed using XRD Goniometer with SHIMADZO-Model XRD 6000. The scanning was done in the region of 2θ from 5° to 80° at 0.02 min, and the time constant was 2 s.

Antioxidant Activity of Ag Nanoparticles

ABTS Scavenging Assay

The total antioxidant activity of AgNPs was evaluated using the Wolfenden and Willson[18] $ABTS^{\bullet+}$ (2,2'-azino-bis (3-ethylbenzothiazoline-6-sulphonic acid) radical cation decolorization test. $ABTS^{\bullet+}$ was created by reacting a 7 mM ABTS aqueous solution with 2.4 mM potassium persulfate. Initially, the mixture was permitted to stand at room temperature for 16 hours in the dark. The incubation mixture contained 0.54 mL of $ABTS^{\bullet+}$, 0.5 mL of phosphate buffer and varying concentrations of sample (20–100 µg GAE) for a total volume of 5 mL. The absorption was measured at 734 nm in the spectrophotometer, and the results were expressed as the equivalent of gallic acid used as a standard. The activity of radical scavenging was expressed as the percentage of free radical inhibition by the sample and measured using the formula: % of ABTS radical scavenging activity = $A_0–A_1/A_0\times100$ Where A_0= absorbance of the control and A_1 =absorbance of the sample.

DPPH Radical Scavenging Assay

Radical scavenging assay of 1.1-diphenyl-2-picryl-hydrazil (DPPH) inhibition in AgNPs was determined by using the standard method.[19] The hydrogen atom or electron donation potential of the sample was determined by bleaching the purple-colored DPPH methanolic solution. One mL of the reaction solution containing 0.1 mmol/l DPPH in methanol was added to the various amounts of samples (20–100 µg) dissolved in 0.5% DMSO and produced up to 3 mL of water. The combination was vigorously agitated for 30 minutes at room temperature before the absorbance of the resultant, solution was measured using a spectrophotometer at 517 nm. Gallic acid was employed as a reference standard for comparison. The following equation was used to measure the inhibition percentage of DPPH radical scavenging activity: % DPPH radical scavenging activity = $A_0–A_1/A_0\times100$ Where A_0 = absorbance of the control and A_1 = absorbance of the sample.

Hydroxyl Radical Scavenging Activity

The hydroxyl radical ($OH^{\bullet}$) scavenging potential was determined using the revised approach of Halliwell et al.[20] For a total volume of 1 mL, the incubation mixture contained 0.1 mL of 100 mM potassium phosphate buffer (pH 7.9) and various amounts of AgNPs (20–100 µg GAE). The assay was performed in distilled deionized water by adding 0.1mL EDTA (1 mM), 0.2 mL $FeCl_3$ (10 mM), 0.1 mL Ascorbic Acid (1 mM), 0.1 mL H_2O_2 (10 mM) and 0.2 mL 2-Deoxyribose (10 mM). After that, the mixture was incubated for 1 hour at 37°C. To generate the pink chromogen detected at 532 nm, 1.0 mL of the incubated mixture was combined with 1.0 mL of 10% TCA and 1.0 mL of 0.5% TBA (in 0.025 M NaOH containing 0.025% BHA). Decreased reaction mixture absorption implies the increased scavenging activity of $OH^{\bullet}$. The compound's hydroxyl radical scavenging activity is stated as percent deoxyribose degradation inhibition and measured using the following equation: Hydroxyl radical scavenging activity = $A_0–A_1/A_0\times100$ Where A_0 = absorbance of control and A_1=absorbance of sample.

Superoxide Radicals Assay

Superoxide anion ($O_2^{\bullet-}$) scavenging activity of AgNPs was determined by the method of Nishikimi et al[21] with slight modifications. In these experiments, 3 mL of Tris-HCl buffer (16 mM, pH 8.0) containing 1 mL of NBT (50 mM) solution, 1 mL of NADH (78 mM) solution and varying amounts of AgNPs (20–100 µg GAE) were used to produce superoxide radicals. The reaction began by adding to the mixture 1 mL of PMS solution (10 mM, pH 7.4). The reaction mixture was incubated for 15 minutes at 30°C, forming a violet color complex indicating superoxide anion production, which was read with the reagent blank at 560 nm. For comparison, Gallic Acid has been used as a reference standard. The increase in superoxide anion scavenging activity was demonstrated by reduced absorption of the reaction mixture. The percent inhibition of the generation of superoxide anion was determined using the following formula: % inhibition = $A_0–A_1/A_0\times100$ where A_0= absorbance of the control and A_1=absorbance of the sample.

Nitric Oxide Radical Scavenging Assay

One mL of the varied concentrations of AgNPs (20–100 g GAE) was mixed with 0.5 mL of sodium nitroprusside (10mM) in phosphate-buffered saline and incubated at 25°C for 150 minutes. Control experiments were carried out in a similar way, using the same amounts of buffer. An equivalent volume of freshly produced Griess reagent was added to the sample (1% sulphanilamide in 2.5% phosphoric acid and 0.1% naphthyl ethylene diamine dihydrochloride in 2.5% phosphoric acid). Gallic acid was employed as a positive control and the absorbance of the chromophore produced was measured at 546 nm. The IC_{50} was calculated, which is the inhibitory concentration of each sample required to limit nitric oxide generation by 50%. Using the formula below, the % nitrite radical scavenging activity of the AgNPs and gallic acid was determined.[22] Percentage nitrite radical scavenging activity: Nitric oxide scavenged % = $A_0–A_1/A_0\times100$ Where A_0= absorbance of control and A_1=absorbance of sample.

Reducing Power Assay

According to Oyaizu's method, the reducing power of the samples was determined.[23] In the test tubes, varying amounts of AgNPs (20–100 g GAE) were mixed with phosphate buffer (2.5 mL, 0.2 M, pH 6.6) and potassium ferricyanide (1%), and the mixture was incubated at 50°C for 20 minutes. After that, 1.5 mL of 10% trichloroacetic acid was added to the reaction mixture, which was centrifuged for 10 minutes at 3000 rpm. The absorbance was measured at 700 nm after the upper layer of the solution (0.5 mL) was combined with distilled water (1 mL) and ferric chloride (0.5 mL, 1%). Gallic acid was employed as a comparison standard.

Anticancer Activity of Ag Nanoparticles

MCF-7 and Caco-2 Cell Line Culture

Breast (MCF-7) and colorectal (Caco-2) cancer cells were purchased from a European collection of authenticated cell cultures (ECACC). Frozen cells were thawed at 37°C and cultured in the Dulbecco's modified Eagle's medium (DMEM, Gibco, USA), supplemented with 10% fetal bovine serum and 1%penicillin/streptomycin (Gibco, USA). After the cells got 70% confluency, the cells were trypsinized, transferred into new tissue culture flasks and maintained at 5% CO_2 in a CO_2 incubator. Cultures of both cell lines were routinely observed under an inverted microscope to evaluate the quantity of confluence and confirm the absence of bacterial and fungal contaminants.

MTT Assay

To determine the cytotoxic effects of the silver nanoparticles of *Moringa* extract, a cell viability study was conducted with the MTT (3-(4,5-dimethylthiazol-2-yl)-2,5-diphenyltetrazolium bromide) reduction assay based on the standard method.[24] Cells were grown in the tissue culture flasks up to 70% of the confluency. Both cell lines were trypsinized and seeded in a 96-well plate at the density of 1×10^4 cells/well. After seeding, the cells in DMEM (10% FBS and 1% Pen/Strep) in the 96 well plates were kept inside the incubator at 37°C for 24 h to attach the cells. After 24 h, the old media were replaced with a new media suspension containing various concentrations of silver nanoparticles 10 to 100 µg/mL. Each concentration was seeded in three wells, and the experiments were duplicated. After the treatment, the cells were incubated for 48 h in a CO_2 incubator. After the treatment was completed, the cells were observed under the microscope and followed by the addition of 25 µL of MTT (5 mg/mL). Then, the microplate was incubated at 37°C for another 4 h. After incubation, the medium was removed, and 200 µL of DMSO was added to each well to dissolve the crystalized formazan. The optical density of the color developed was examined at 570 nm wavelength with a Thermo Scientific multi-scan geo spectrophotometer. OD value was used to calculate the percentage of viability by using the following formula, Percentage of cell viability = OD of Sample/OD of Control × 100.

Statistical Analysis

The antioxidant assay experiments were performed in triplicates, and the values were expressed in mean ± SD. The SPSS (11.5) package was used for the statistical analysis. One-way analysis of variance and Duncan's multiple range tests were performed to determine the significance between the means. Anticancer results were expressed as a mean percentage ± standard deviation (SD) of the mean negative control (untreated cells) absorbance. Then the viability percentage was

calculated with absorbance data. These data were analyzed using GraphPad Prism software which was used to construct dose response curves of the various extracts on the cells.

Results

Characterization of Nanoparticles

FT-IR Spectral Analysis

The FT-IR spectrum of *Moringa peregrina*-mediated AgNPs is shown in Figure 2. The absorption bands at approximately 3300 cm^{-1} are assigned to the presence of minor moisture. An additional band identified in the range between 2800 cm^{-1} and 2950 cm^{-1} can be assigned to the C–H asymmetric stretching vibration mode. The prominent band detected around 1600 cm^{-1} corresponds to the stretching vibration mode of O–H. The bands at approximately 1045 cm^{-1} are associated with the vibrations of hydroxyl O–H groups. The low-frequency band at 517.5 cm^{-1} can be attributed to the intrinsic vibrations of the transition metal Ag band position in the silver nanoparticles (AgNPs).

In the present investigation, the donor of electrons is *Moringa peregrina* leaf aqueous extract, and the acceptor was Ag^{+} ions in aqueous silver nitrate solution. From this observation, it is suggested that the reduction of Ag^{+} ions into Ag^{0} depends on the Van der Waals interactions between the supplier and the acceptor.

HR-SEM and EDX Studies

The particle size and the purity of AgNPs can be illustrated by SEM and EDX analyses. Figure 3 represents the SEM image of AgNPs synthesized by the *Moringa peregrina* leaf extract and confirms the particle in the range of 30–35 nm. The SEM images indicate that the AgNPs exhibit strong connectivity among their grains, suggesting agglomeration. This agglomeration is ascribed to Van der Waals forces. The present EDX analysis depicted in Figure 4 shows a high percentage of Ag indicating the purity of the synthesized sample. The EDX spectrum also reveals that the major peak is due to the metallic Ag confirming the formation of AgNPs.

HR-TEM Analysis

The morphology and size of the synthesized AgNPs by *Moringa peregrina* leaf extract are characterized by HR-TEM images as shown in Figure 5. The HR-TEM images confirm the particle size of AgNPs ranging from 25 to 60 nm. The silver nanoparticles (AgNPs) exhibited predominantly spherical particles, with a relatively lower degree of particle agglomeration. Hence, this result is consistent with the SEM findings.

XRD Studies

The crystalline nature of the biosynthesized AgNPs was determined by XRD analysis as illustrated in Figure 6. The observed diffraction peaks at 2θ values of 27.9, 32.4, 38.4, 44.6, 46.8, 54.9, 57.6, 64.3, and 77.9. These values

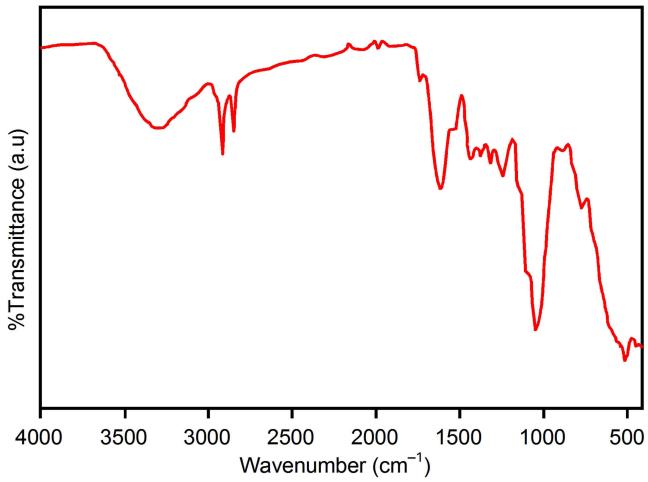

Figure 2 FT-IR spectrum of AgNPs synthesized with *M. peregrina* leaf extract.

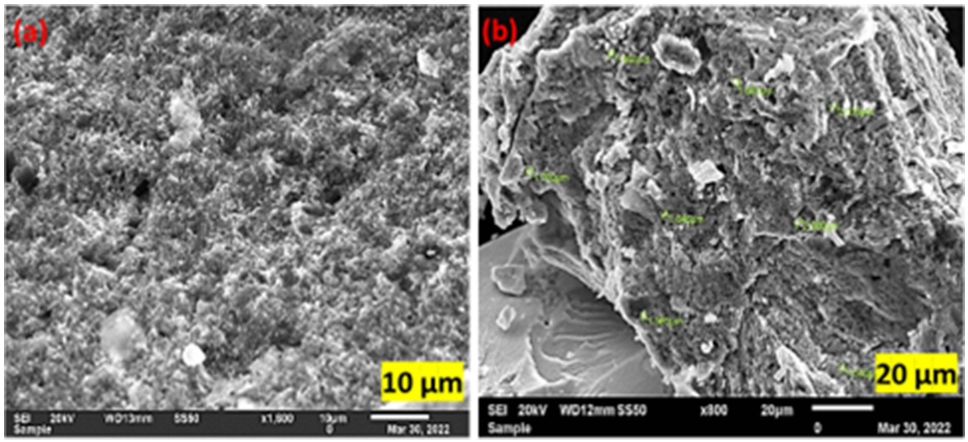

Figure 3 HR-SEM image of AgNPs synthesized by *M. peregrina* leaf extract at different scales: (**a**) 10 µm and (**b**) 20 µm.

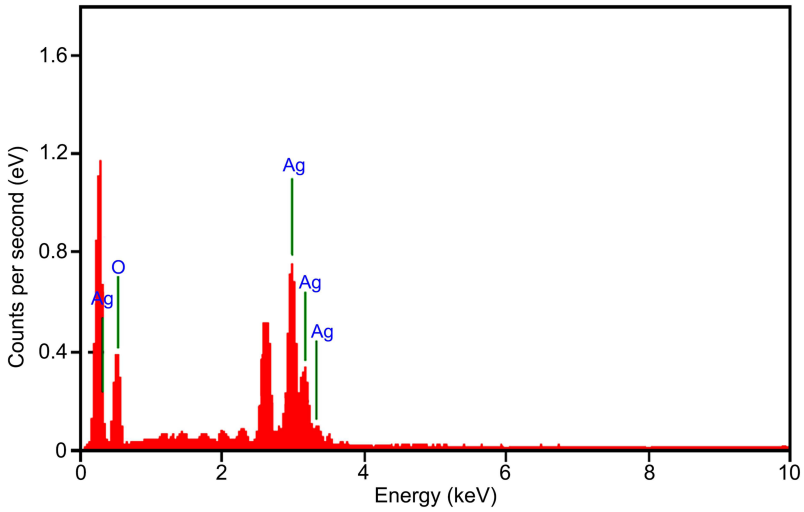

Figure 4 EDX spectrum of AgNPs synthesized using *M. peregrina* leaf extract.

correspond with Miller plane indices of (210), (122), (111), (200), (231), (142), (241), (220) and (311), respectively. The results show a good agreement with standard data (JCPDS: 04–0783) and the studies provide strong evidence that synthesized AgNPs have a face-centered cubic (FCC) structure of the metallic silver. No discernible additional diffraction peaks were observed in the XRD patterns. This suggests the high purity of the biosynthesized silver nanoparticles (AgNPs).

Antioxidant Activity

ABTS Radical Scavenging Activity

The tuber part of the plant extracts was fast and effective scavengers of the ABTS radical (Figure 7a), and this activity was comparable to that of GA. The percentage of inhibition was 57% and 68% for AgNPs and GA, respectively, at 100 µg/mL concentration. In $ABTS^{+}$ scavenging activity the values varied significantly ($P < 0.05$) and ranged from 20 to 100 µg GA/g extract. The ABTS radical cation scavenging activity also reflects hydrogen-donating ability.

DPPH Free Radical Scavenging Activity

The antioxidant activity of the $AgNO_3$ is shown in Figure 7b as the DPPH inhibition percentage. The silver nanoparticles were a potent-free radical scavenger when compared with the Gallic acid standard. The antioxidant activity of the nanoparticles was 73% inhibition at 100 mg/mL and that for ascorbic acid was 62% inhibition. The essence of the DPPH

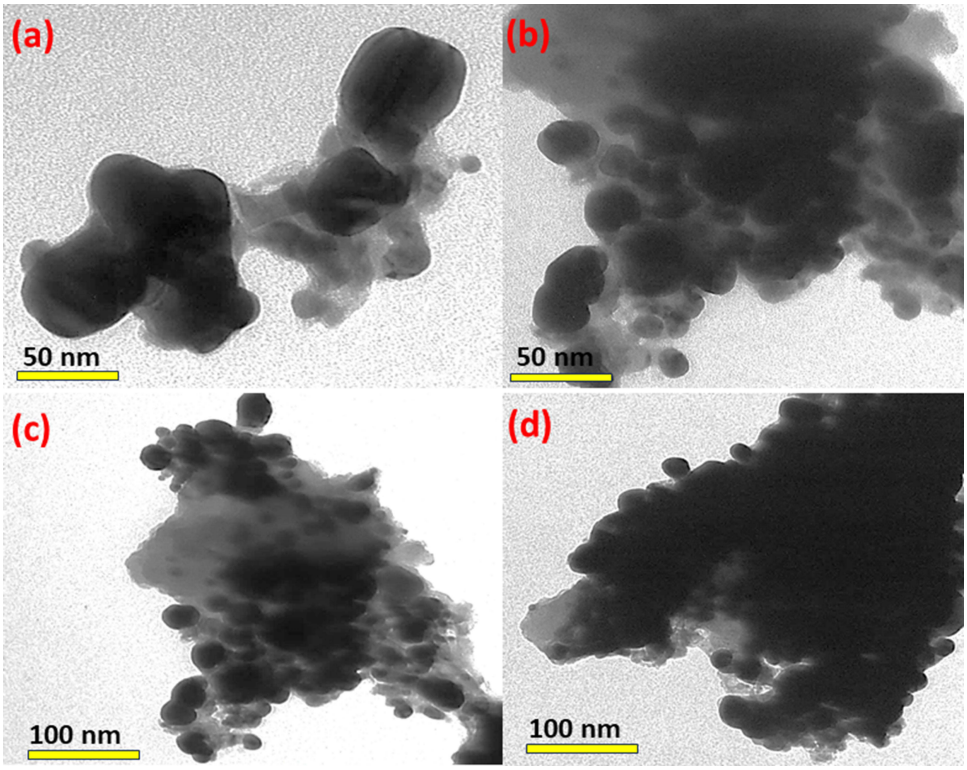

Figure 5 HR-TEM image of AgNPs at different magnifications: (**a** and **b**) 50 nm and (**c** and **d**) 100 nm of synthesized using *M. peregrina* leaf extract.

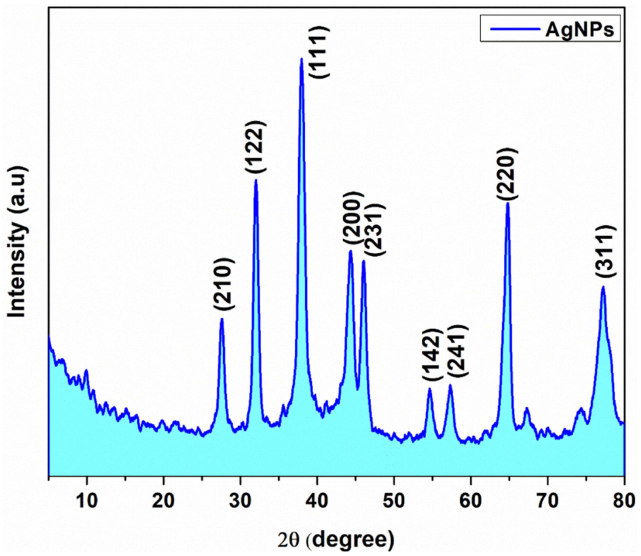

Figure 6 XRD patterns of AgNPs.

method is that the antioxidants react with the stable free radical, ie, α, α diphenyl-β-picrylhydrazyl (deep violet color) and convert it to α, α-diphenyl-β-picrylhydrazine with discoloration. Compared to GA, the AgNPs exhibited a high level of antioxidant activity.

Hydroxyl Radical Scavenging Activity

The percentage of hydroxyl radical-scavenging activity of AgNPs at various concentrations is presented in Figure 7c. The AgNPs and GA showed significant inhibitory activity in a concentration-dependent manner. The potential of

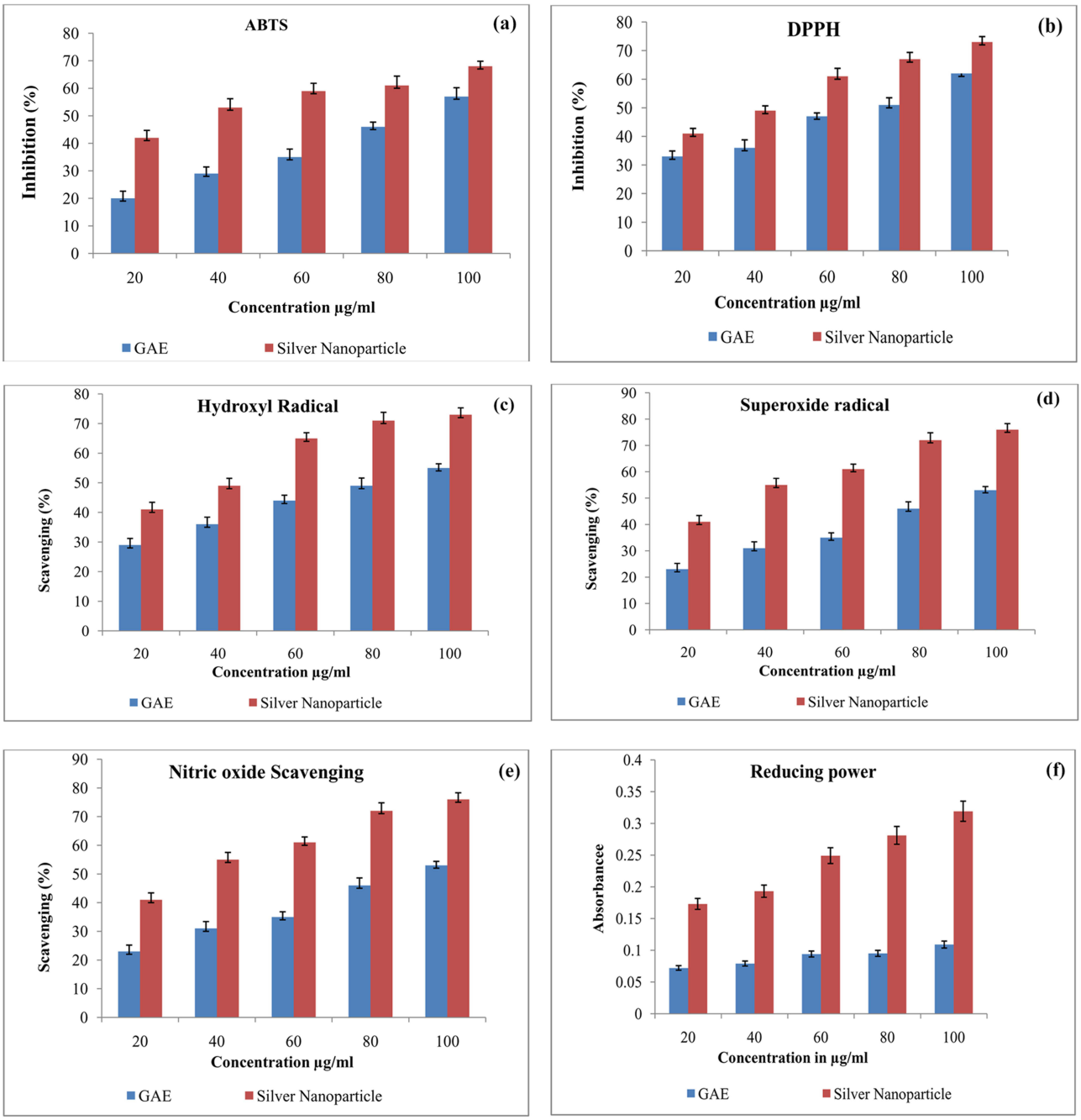

Figure 7 Antioxidant potential of AgNPs using *M. peregrina* leaf extract. (**a**) ABTS free radical scavenging activity; (**b**) DPPH radical scavenging activity' (**c**) Hydroxyl radical scavenging; (**d**) Superoxide radical scavenging activity; (**e**) Nitric oxide radical scavenging activity; (**f**) Reducing power of AgNP; "GAE"- Gallic acid; Values are presented as means±standard deviation.

AgNPs to inhibit hydroxyl-radical-mediated deoxyribose damage was assessed at a concentration of 10–100 µg/mL. AgNPs showed the maximum inhibition (73%) at 100 µg and the concentration needed for 50% inhibition was 60 µg GA.

Superoxide Radicals Scavenging Activity

At 10–100 µg/mL, the superoxide scavenging activity of AgNPs was 34–76%, and that of the standard gallic acid was 23–53%. The superoxide scavenging activity of AgNPsand standard gallic acid is shown in Figure 7d. AgNPs

exhibited concentration-dependent radical scavenging activity, that is, inhibition percentage increased with sample concentration.

Nitric Oxide Scavenging

The scavenging of nitric oxide of AgNPs increased in a dose-dependent manner. The $AgNO_3$ showed good nitric oxide scavenging activity (Figure 7e) at the concentration of 40 µg when compared to standard GA.

Reducing Power

Figure 7f shows the reductive capabilities of AgNPs at different concentrations, ranging from 10 to 100 µg/mL compared to GA. The AgNPs exhibited a significant dose-dependent inhibition of reducing power-scavenging activity, with a 50% inhibition. The reducing power of AgNPs was very potent, and the reducing power of the nanoparticles was increased with the quantity of sample. The AgNPs could reduce the most Fe^{3+} ions, which had a lesser reductive activity than the standard of GA. The $AgNO_3$ synthesized by the extract of *M. peregrina* exhibited significant dose-dependent inhibition of reducing power activity.

Anticancer Activity

Anti-cancer activity of phytochemical mediated nanoparticles is getting attracted due to increasing interest as silver nanoparticles being considered as novel agents. Our study aimed to detect the anti-cancer activity of the silver nanoparticles from the *Moringa* leaf extract. In this study, we used two types of cancer cell lines (Caco-2 and MCF-7). Our results showed that low concentrations of the nanoparticles were very effective against cancer cells under in vitro conditions. The cell death increased upon increasing the concentration of the nanoparticles from 10 to 1000µg/mL. In our earlier studies, various leaf extracts showed cell death with high concentration only (above 100 µg/mL), but *Moringa* leaf nanoparticles showed a much better cell death rate compared to the crude extract.

Cell viability of the Caco-2 cells and MCF-7 after exposure to different concentrations of *Moringa* nanoparticles is plotted by percentage viability on the y-axis and nanoparticle concentration on the x-axis in the graph Figure 8A and B, respectively. Doxorubicin was used as a control for these experiments and plotted in Figure 8C for Caco-2 and Figure 8D for the MCF-7 cell line. When we compared the anticancer activity of the nanoparticles on Caco-2 and MCF-7 cells, no significant variation in the effectiveness of inducing cell death was found, and almost a similar pattern of death was observed with the same concentration. Nevertheless, more death of cells can be noticed with 1000 µg/mL of nanoparticles on MCF-7 cells compared to Caco-2 cells.

GraphPad Prism software was used to perform non-linear regression analysis for the effects of the nanoparticles of the extracts on the MCF-7 and Caco-2 cells in order to determine IC_{50} values. The concentration of nanoparticles on each cell line at which 50% of the cells that were inhibited are shown in Table 1. IC_{50} of the positive control, doxorubicin on both cell lines are also shown in Table 1. There was only a slight variation in the IC_{50} concentration on both types of cell lines where MCF-7 gave better IC_{50} than the Caco-2 cell line.

Discussion

Green Synthesis of Silver Nanoparticles

Nowadays, the synthesis of nanoparticles using plant materials as a reducing and capping agent is gaining attention.[25,26] The identification of color is a preliminary analysis to confirm the formation of AgNPs. It may be because of the excitation of the Surface Plasmon Resonance (SPR) effect and the reduction of $AgNO_3$.[27] The intensity of the brown color increases in direct proportion to the incubation period. In the present study, the complete color change was observed after 2 h. It is well known that the presence of phytochemical components in plants is responsible for the rapid reduction of silver nanoparticles. Usually, the green-synthesized AgNPs have a large surface area which increases the adsorption of bioactive compounds. So, high antioxidant activity was observed in the present study. The phytochemicals involved in the process of green synthesis of nanoparticles are flavonoids, terpenoids, ketones, amides, aldehydes, saponins, carboxylic acids, and organic acids. Moreover, the water-soluble phytoconstituent of quinine is mainly involved in the immediate reduction of silver nitrate. It was reported that the extracts of basil took 1 h to synthesize the AgNPs.[28] Rhizome extracts of *Alpinia calcarata* showed the formation of a brownish-orange color in 5 min, whereas the AgNPs

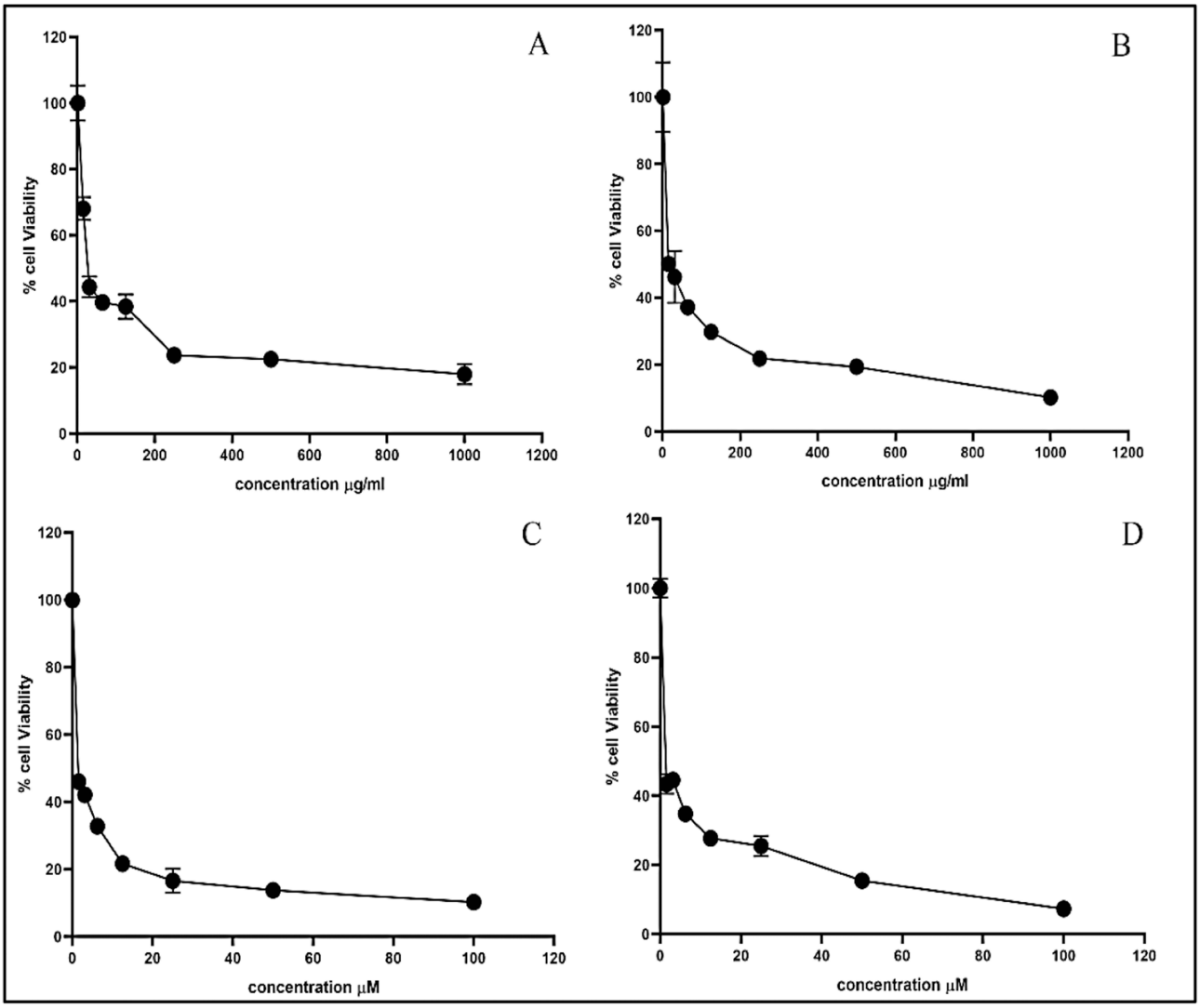

Figure 8 Viability percentage of cancer cells treated with AgNPs and Doxorubicin as a positive control. (**A**) Nanoparticles on Caco-2; (**B**) Nanoparticles on MCF-7; (**C**) Doxorubicin on Caco-2; (**D**) Doxorubicin on MCF-7.

were formed in 10 min when *Azadirachta indica* extracts were used as a reduction agent.[29] This indicates that the intensity of brown color increases with the increase in the duration of incubation.

Antioxidant Activity

In the present study, the green-synthesized nanoparticles using leaf aqueous extract of *M. peregrina* showed effective antioxidant activity in terms of DPPH radical scavenging activity, hydroxyl radical scavenging assay, superoxide anion

Table 1 Anticancer Activity of $AgNO_3$ Nano-Particles on Caco-2 and MCF-7 Cell Lines

Name of the sample	Cell line	IC_{50}
$AgNO_3$ nanoparticle	Caco-2 MCF-7	41.59 µg/mL 26.93 µg/mL
Doxorubicin (Positive Control)	Caco-2 MCF-7	0.74 µg/mL 1.725 µg/mL

radical scavenging assay, nitric oxide radical scavenging assay and reducing power ability at a maximum concentration of 100 µg/mL. The same concentrations of gallic acid were used as a standard for comparison. Surprisingly, in the present study, the AgNPs prepared by the aqueous leaf extract of *M. peregrina* exhibited comparatively excellent antioxidant potential than gallic acid due to the structure and characterization of the AgNPs. These results are in agreement with the previous studies on the antioxidant potential of the green-synthesized AgNPs. Govindappa et al[30] reported the antioxidant activity, *viz*., DPPH, nitric oxide scavenging power, H_2O_2 scavenging and reducing the power of AgNPs prepared by using the aqueous leaf extract of *Calophyllum tomentosum*. Different concentrations *viz*. 10, 20, 30, 40, 50, 75 and 100 µg/mL were prepared and used for the study. The results indicated that the AgNPs had good DPPH scavenging potential compared with BHT. The highest concentration of AgNPs (100 µg/mL) had more inhibition with 90% DPPH scavenging activity and 83.94% H_2O_2 radical scavenging activity. In addition, the AgNPs prepared using aqueous leaf extract of *Calophyllum tomentosum* showed 78.46% inhibition which was less than standard gallic acid (79.11%). According to Jalilian et al,[31] the AgNPs synthesized using hot water extract of *Allium ampeloprasum* showed significant antioxidant potential with the inhibition of 81% at a concentration of 150 µg/mL. In addition, Govindaraju et al[32] reported that the green-synthesized AgNPs have antioxidant potential in a dose-dependent manner. Vijayan et al[33] also obtained similar results from the biosynthesized AgNPs using *Indigofera tinctoria* leaf extract. Usually, the antioxidant properties of the biosynthesized AgNPs are due to their ability as a reducing and stabilizing agent during biosynthesis, being a natural antioxidant material, resulting in the surface modification of AgNPs.[34–36]

Anticancer Activity

Recently, several studies have reported that the green-synthesized AgNPs can be used as an anticancer agent due to their toxic potential on cancer cells.[37,38] Furthermore, in the present scenario, remarkable interest in the anticancer properties of natural product-derived nanoparticles has been seen. Conventional cancer therapies such as chemotherapy and radiation result in serious side effects in addition to the drug resistance of certain cancer cells. These reasons encouraged scientists to focus on natural products and derived nanoparticles therefrom the fight against cancer.[39] Silver nanoparticles are used as antimicrobial agents and antioxidants and also have low toxicity in nature.[40] Cancer cell models are normally used to identify the potent effect of the natural product on inhibiting cancer growth and death of the cells.[41]

In the present study, we preferred MTT as a dye in the anticancer activity test to avoid the cross-coloring of the nanoparticles, with other dissolving dyes. In the case of MTT assay, the addition of formazan crystals will dissolve only with the addition of dimethyl sulphoxide and form a blue-colored product. Formation of the formazan appears only in the living cells and not in the dead cells, so the color developed is measured with spectrophotometry.

In previous reports, the nanoparticles developed from the bark of *Moringa* showed that IC_{50} on the HELA cells reached 100 µg/mL,[42] but in our studies, AgNPs showed better IC_{50} values on breast cancer cells and colorectal cancer cell lines. Here, we report IC_{50} values of 26.93 µg/mL on MCF-7, which is significant when compared to the effect of other extract-synthesized nano-particles such as *Syzygium aromaticum* inducing IC_{50} higher than 50 µg/mL.[43] Silver nanoparticles prepared from the extract of *Moringa*-treated cells showed a significant level of cell death in both cell lines compared to the control cells. Changes in the population of viable cells indicate that the cancer cell death is due to AgNP-inducing antitumor activities. Even though nanoparticles express high antioxidant capacity, the prevalence of cell death in cancer cells indicates that free radical-independent cell signaling is the prime cause of anti-cancerous activity. Most of the previous research studies suggest that oxidative stress generated by reactive oxygen species is the primary factor behind cellular toxicity and cell death cells.[44] Also, by altering crucial signaling pathways, such as the hypoxia-inducible factor, silver nanoparticles may induce apoptosis by up or down-regulating the expression of important genes, such as p53.[45,46] Morphological changes in the MCF-7 and Caco-2 cells during the treatment with nanoparticles provide insights indicating that the cell death is likely attributed to apoptosis rather than necrosis.[47] Upon exposure of cancer cell lines to AgNPs, it experiences sub-G1 arrest and apoptosis. By inhibiting tumor cell migration and angiogenesis, silver nanoparticles may also diminish distant metastasis.[48,49]

Conclusion

In recent years, the green-synthesized nanoparticles have found various biochemical applications including but not limited to acting as an antioxidant, anticancer, antimicrobial, antiviral, anti-inflammatory, cytotoxic and anti-HIV agents. Furthermore, AgNPs are extensively used for the drug delivery, diagnosis and treatment of diseases because of their biological activity and being eco-friendly and nontoxic to humans. In that way, silver nanoparticles synthesized using *Moringa peregrina* aqueous leaf extract showed good antioxidant potential and anticancer activity against human cancer cell lines (Caco-2 and MCF-7). The biosynthesized nanoparticles using *M. peregrina* leaf extract as a reducing agent exhibited promising antioxidant and anticancer potential on human cancer cells, making them suitable for potential biological applications. The effect of these nanoparticles on normal cells is not investigated in the present study. Therefore, further investigations into the effect of AgNPs on normal cell lines, surface modification of AgNPs during biosynthesis, and a deeper exploration of the signaling mechanisms underpinning their actions are essential to gain a more comprehensive understanding of their bioactivity.

Acknowledgments

Author K.S.Y.A.B. as part of his Master of Science in Horticulture Degree in Department of Integrative Agriculture at UAEU, under the major supervision of A.J. and co-supervision of A.S.O.S.A.D. and M.A.M.A. The assistance from staff of Al Foah Experimental Station and E3, F1 labs, CAVM, and UAEU is greatly acknowledged.

Funding

This research was funded by UAEU, UPAR#31F092.

Disclosure

This paper is based on the MS Horticulture thesis of Mr. Khaled Saeed Yousef Al Baloushi (first author of this article) under the supervision of Dr. Abdul Jaleel (Corresponding author of this article) and co-supervision of Dr. Mohammed Abdul Muhsen Alyafei and Prof. Ayesha Salem Al Dhaheri (Authors in this article). It has been published on the institutional website: https://scholarworks.uaeu.ac.ae/all_theses/1041/.

References

1. Bayda S, Adeel M, Tuccinardi T, Cordani M, Rizzolio F. The history of nanoscience and nanotechnology: From chemical-physical applications to nanomedicine. *Molecules*. 2019;25(1):112. doi:10.3390/molecules25010112
2. Jo HJ, Choi JW, Lee SH, Hong SW. Acute toxicity of Ag and CuO nanoparticle suspensions against *Daphnia magna*: The importance of their dissolved fraction varying with preparation methods. *J Hazard Mater*. 2012;227-228:301–308. doi:10.1016/j.jhazmat.2012.05.066
3. Selim YA, Azb MA, Ragab I, Abd El-Azim M HM. Green synthesis of zinc oxide nanoparticles using aqueous extract of *Deverra tortuosa* and their cytotoxic activities. *Sci Rep*. 2020;10(1):3445. doi:10.1038/s41598-020-60541-1
4. Hou T, Guo Y, Han W, et al. Exploring the biomedical applications of biosynthesized silver nanoparticles using *Perilla frutescens* flavonoid extract: antibacterial, antioxidant, and cell toxicity properties against colon cancer cells. *Molecules*. 2023;28(17):6431. doi:10.3390/molecules28176431
5. Stafford S, Serrano Garcia R, Gun'ko YK. Multimodal magnetic-plasmonic nanoparticles for biomedical applications. *Applied Sci*. 2018;8(1):97. doi:10.3390/app8010097
6. Idrees H, Zaidi SZJ, Sabir A, Khan RU, Zhang X, Hassan SU. A review of biodegradable natural polymer-based nanoparticles for drug delivery applications. *Nanomaterials*. 2020;10(10):1970. doi:10.3390/nano10101970
7. Sreekanth TVM, Pandurangan M, Kim DH, Le YR. Green synthesis: In-vitro anticancer activity of silver nanoparticles on human cervical cancer cells. *J Clust Sci*. 2016;27:671–681. doi:10.1007/s10876-015-0964-9
8. Ranjitham AM, Suja R, Carolling G, Tiwari S. *In vitro* evaluation of antioxidant antimicrobial, anticancer activities and characterization of *Brassica oleracea* Var. *botrytis* L synthesized silver nanoparticles. *Intl J Pharma Biosci*. 2013;5(4):239–251.
9. Sukanya SL, Sudisha J, Niranjana SR, Prakash HP, Fathima SK. Antimicrobial activity of leaf extract of India medicinal plants against clinical and phytopathogenic bacteria. *Afr J Biotechnol*. 2009;8(23):6677–6682.
10. Hernández HH, Benavides-Mendoza A, Ortega-Ortiz H, Hernández-Fuentes AD, Juárez-Maldonado A. Cu nanoparticles in chitosan-PVA hydrogels as promoters of growth, productivity and fruit quality in tomato. *Emir J Food Agric*. 2017;29(8):573–580. doi:10.9755/ejfa.2016-08-1127
11. Siva PK, Sathish M, Parvathi T, Kamaraj M, Bhuvaneswari R, Arumugam M. Green synthesis of silver nanoparticles using *Indigofera cordifolia* leaf extract and their pharmacological potential. *J Phytol*. 2021;13:48–54. doi:10.25081/jp.2021.v13.7048
12. Kar P, Banerjee S, Chhetri A, Sen A. Synthesis, physicochemical characterization and biological activity of synthesized Silver and Rajat Bhasma nanoparticles using *Clerodendrum inerme*. *J Phytol*. 2021;1:64–71. doi:10.25081/jp.2021.v13.7026
13. Salayová A, Bedlovičová Z, Daneu N, et al. Green synthesis of silver nanoparticles with antibacterial activity using various medicinal plant extracts: Morphology and antibacterial efficacy. *Nanomaterials*. 2021;11(4):1005. doi:10.3390/nano11041005

14. Olson ME. Combining data from DNA sequences and morphology for a phylogeny of moringaceae (brassicales). *Syst Bot*. 2002;27(1):55–73. doi:10.1043/0363-6445-27.1.55
15. Salaheldeen M, Aroua MK, Mariod AA, Cheng SF, Abdelrahman MA. An evaluation of *Moringa peregrina* seeds as a source for bio-fuel. *Ind Crops Prod*. 2014;61:49–61. doi:10.1016/j.indcrop.2014.06.027
16. Senthilkumar A, Karuvantevida N, Rastrelli L, Kurup SS, Cheruth AJ. Traditional uses, pharmacological efficacy, and phytochemistry of *Moringa peregrina* (forssk.) fiori-A Review. *Front Pharmacol*. 2018;9:465. doi:10.3389/fphar.2018.00465
17. Mahadevan S, Vijayakumar S, Arulmozhi P. Green synthesis of silver nano particles from *Atalantia monophylla* (L) Correa leaf extract, their antimicrobial activity and sensing capability of H_2O_2. *Microb Pathog*. 2017;113:445–450. doi:10.1016/j.micpath.2017.11.029
18. Wolfenden BS, Willson RL. Radical-cations as reference chromogens in kinetic studies of ono-electron transfer reactions: pulse radiolysis studies of 2, 2′-azinobis-(3-ethylbenzthiazoline-6-sulphonate). *J Chem Soc, Perkin Trans*. 1982;27:805–812. doi:10.1039/P29820000805
19. Brand-Williams W, Cuvelier ME, Berset C. Use of free radical method to evaluate the antioxidant activity. *LWT - Food Sci Technol*. 1995;28:25–30. doi:10.1016/S0023-6438(95)80008-5
20. Halliwell B, Gutteridge JM, Aruoma OI. The deoxyribose method: a simple ”test-tube” assay for determination of rate constants for reactions of hydroxyl radicals. *Anal Biochem*. 1987;165(1):215–219. doi:10.1016/0003-2697(87)90222-3
21. Nishikimi M, Appaji N, Yagi K. The occurrence of superoxide anion in the reaction of reduced phenazine methosulfate and molecular oxygen. *Biochem Biophys Res Commun*. 1972;46(2):849–854. doi:10.1016/s0006-291x(72)80218-3
22. Green LC, Wagner DA, Glogowski J, Skipper PL, Wishnok JS, Tannenbaum SR. Analysis of nitrate, nitrite, and [15N]nitrate in biological fluids. *Anal Biochem*. 1982;126(1):131–138. doi:10.1016/0003-2697(82)90118-x
23. Oyaizu M. Studies on products of browning reactions: Antioxidative activities of products of browning reaction prepared from glucosamine. *Japanese J Nutr Diet*. 1986;44:307–315. doi:10.5264/eiyogakuzashi.44.307
24. Del Peso L, González-García M, Page C, Herrera R, Nuñez G. Interleukin-3-induced phosphorylation of BAD through the protein kinase akt. *Science*. 1997;278(5338):687–689. doi:10.1126/science.278.5338.687
25. Skóra B, Szychowski KA, Gmiński J. A concise review of metallic nanoparticles encapsulation methods and their potential use in anticancer therapy and medicine. *Eur J Pharm Biopharm*. 2020;154:153–165. doi:10.1016/j.ejpb.2020.07.002
26. Vaid P, Raizada P, Saini AK, Saini RV. Biogenic silver, gold and copper nanoparticles - A sustainable green chemistry approach for cancer therapy. *Sustain Chem Pharm*. 2020;16:100–247. doi:10.1016/j.scp.2020.100247
27. Mulvaney P. Surface plasmon spectroscopy of nanosized metal particles. *Langmuir*. 1996;12(3):788–800. doi:10.1021/la9502711
28. Ahmad N, Sharma S, Alam MK, et al. Rapid synthesis of silver nanoparticles using dried medicinal plant of basil. *Colloids Surf B*. 2010;81(1):81–86. doi:10.1016/j.colsurfb.2010.06.029
29. Shankar SS, Rai A, Ahmad A, Sastry M. Rapid synthesis of Au, Ag, and bimetallic Au core-Ag shell nanoparticles using neem (*Azadirachta indica*) leaf broth. *J Colloid Interface Sci*. 2004;275(2):496–502. doi:10.1016/j.jcis.2004.03.003
30. Govindappa M, Hemashekhar B, Arthikala MK, Rai VR, Ramachandra YL. Characterization, antibacterial, antioxidant, antidiabetic, anti-inflammatory and antityrosinase activity of green synthesized silver nanoparticles using *Calophyllum tomentosum* leaves extract. *Res Physics*. 2018;9:400–408. doi:10.1016/j.rinp.2018.02.049
31. Jalilian F, Chahardoli A, Sadrjavadi K, Fattahi A, Shokoohinia Y. Green synthesized silver nanoparticle from *Allium ampeloprasum* aqueous extract: Characterization, antioxidant activities, antibacterial and cytotoxicity effects. *Adv Powder Tech*. 2020;31(3):1323–1332. doi:10.1016/j.apt.2020.01.011
32. Govindaraju K, Krishnamoorthy K, Alsagaby SA, Singaravelu G, Premanathan M. Green synthesis of silver nanoparticles for selective toxicity towards cancer cells. *IET Nanobiotechnol*. 2015;9(6):325–330. doi:10.1049/iet-nbt.2015.0001
33. Vijayan R, Joseph S, Mathew B. *Indigofera tinctoria* leaf extract mediated green synthesis of silver and gold nanoparticles and assessment of their anticancer, antimicrobial, antioxidant and catalytic properties. *Artif Cells Nano Biotech*. 2018;46(4):861–871. doi:10.1080/21691401.2017.1345930
34. Kanagalakshmi K, Premanathan M, Priyanka R, Hemalatha B, Vanangamudi A. Synthesis, anticancer and antioxidant activities of 7-methoxyisoflavanone and 2,3-diarylchromanones. *Eur J Med Chem*. 2010;45(6):2447–2452. doi:10.1016/j.ejmech.2010.02.028
35. Premanathan M, Karthikeyan K, Jeyasubramanian K, Manivannan G. Selective toxicity of ZnO nanoparticles toward gram-positive bacteria and cancer cells by apoptosis through lipid peroxidation. *Nanomedicine*. 2011;7(2):184–192. doi:10.1016/j.nano.2010.10.001
36. Veeraapandian S, Sawant SN, Doble M. Antibacterial and antioxidant activity of protein capped silver and gold nanoparticles synthesized with *Escherichia coli*. *J Biomed Nanotechnol*. 2012;8(1):140–148. doi:10.1166/jbn.2012.1356
37. Mohanta YK, Panda SK, Biswas K, et al. Biogenic synthesis of silver nanoparticles from *Cassia fistula* (Linn.): In vitro assessment of their antioxidant, antimicrobial and cytotoxic activities. *IET Nanobiotechnol*. 2016;10(6):438–444. doi:10.1049/iet-nbt.2015.0104
38. Singh H, Du J, Singh P, Yi TH. Ecofriendly synthesis of silver and gold nanoparticles by *Euphrasia officinalis* leaf extract and its biomedical applications. *Artif Cells Nanomed Biotechnol*. 2018;46(6):1163–1170. doi:10.1080/21691401.2017.1362417
39. Velpurisiva P, Gad A, Piel B, Jadia R, Rai P. Nanoparticle design strategies for effective cancer immunotherapy. *J Biomed*. 2017;2(2):64–77. doi:10.7150/jbm.18877
40. Kim JS, Kuk E, Yu KN, et al. Antimicrobial effects of silver nanoparticles. *Nanomedicine*. 2007;3(1):95–101. doi:10.1016/j.nano.2006.12.001
41. Kim CG, Castro-Aceituno V, Abbai R, et al. Caspase-3/MAPK pathways as main regulators of the apoptotic effect of the phyto-mediated synthesized silver nanoparticle from dried stem of *Eleutherococcus senticosus* in human cancer cells. *Biomed Pharmacother*. 2018;99:128–133. doi:10.1016/j.biopha.2018.01.050
42. Vasanth K, Ilango K, MohanKumar R, Agrawal A, Dubey GP. Anticancer activity of *Moringa oleifera* mediated silver nanoparticles on human cervical carcinoma cells by apoptosis induction. *Coll Surf B Biointerfaces*. 2014;117:354–359. doi:10.1016/j.colsurfb.2014.02.052
43. Venugopal K, Rather HA, Rajagopal K, et al. Synthesis of silver nanoparticles (Ag NPs) for anticancer activities (MCF 7 breast and A549 lung cell lines) of the crude extract of *Syzygium aromaticum*. *J Photochem Photobiol B*. 2017;167:282–289. doi:10.1016/j.jphotobiol.2016.12.013
44. Johnston HJ, Hutchison G, Christensen FM, Peters S, Hankin S, Stone V. A review of the *in vivo* and *in vitro* toxicity of silver and gold particulates: particle attributes and biological mechanisms responsible for the observed toxicity. *Crit Rev Toxicol*. 2010;40(4):328–346. doi:10.3109/10408440903453074
45. Yuan YG, Zhang S, Hwang JY, Kong IK. Silver nanoparticles potentiates cytotoxicity and apoptotic potential of camptothecin in human cervical cancer cells. *Oxid Med Cell Longev*. 2018;6121328. doi:10.1155/2018/6121328

46. Mohamed AF, Nasr M, Amer ME, et al. Anticancer and antibacterial potentials induced post short-term exposure to electromagnetic field and silver nanoparticles and related pathological and genetic alterations. *Vitro Study Infect Agent Canc*. 2022;17(1):4. doi:10.1186/s13027-022-00416-4
47. Saraste A, Pulkki K. Morphologic and biochemical hallmarks of apoptosis. *Cardiovasc Res*. 2000;45(3):528–537. doi:10.1016/s0008-6363(99)00384-3
48. Noorbazargan H, Amintehrani S, Dolatabadi A, et al. Anti-cancer & anti-metastasis properties of bioorganic-capped silver nanoparticles fabricated from *Juniperus chinensis* extract against lung cancer cells. *AMB Express*. 2021;11(1):61. doi:10.1186/s13568-021-01216-6
49. Kitimu SR, Kirira P, Abdille AA, et al. Anti-angiogenic and anti-metastatic effects of biogenic silver nanoparticles synthesized using *Azadirachta indica*. *Adv Biosci Biotechnol*. 2022;13:188–206. doi:10.4236/abb.2022.134010